A Circular-Structured Representation for Visual Emotion Distribution Learning

Jingyuan Yang[1]   Jie Li[1]   Leida Li[2]   Xiumei Wang[1]   Xinbo Gao[1,3*]

[1] School of Electronic Engineering, Xidian University, Xi'an, China
[2] School of Artificial Intelligence, Xidian University, Xi'an, China
[3] The Chongqing Key Laboratory of Image Cognition,
Chongqing University of Posts and Telecommunications, Chongqing, China

jingyuanyang@stu.xidian.edu.cn, leejie@mail.xidian.edu.cn, ldli@xidian.edu.cn,
wangxm@xidian.edu.cn, xbgao@mail.xidian.edu.cn

Abstract

Visual Emotion Analysis (VEA) has attracted increasing attention recently with the prevalence of sharing images on social networks. Since human emotions are ambiguous and subjective, it is more reasonable to address VEA in a label distribution learning (LDL) paradigm rather than a single-label classification task. Different from other LDL tasks, there exist intrinsic relationships between emotions and unique characteristics within them, as demonstrated in psychological theories. Inspired by this, we propose a well-grounded circular-structured representation to utilize the prior knowledge for visual emotion distribution learning. To be specific, we first construct an Emotion Circle to unify any emotional state within it. On the proposed Emotion Circle, each emotion distribution is represented with an emotion vector, which is defined with three attributes (i.e., emotion polarity, emotion type, emotion intensity) as well as two properties (i.e., similarity, additivity). Besides, we design a novel Progressive Circular (PC) loss to penalize the dissimilarities between predicted emotion vector and labeled one in a coarse-to-fine manner, which further boosts the learning process in an emotion-specific way. Extensive experiments and comparisons are conducted on public visual emotion distribution datasets, and the results demonstrate that the proposed method outperforms the state-of-the-art methods.

1. Introduction

Emotion serves as one of the most essential factors that distinguish human beings from other species, which affects almost every aspect of our daily lives. With the prevalence of social networks, more and more people tend to express their feelings by sharing images on the internet. There-

Figure 1. Four images with different emotion distributions from the involved datasets. Rather than a dominant emotion, images often evoke multiple emotions with different description degrees.

fore, *Visual Emotion Analysis (VEA)* has drawn great attention recently, which aims at understanding how people feel emotionally towards different visual stimuli. The development in VEA may also bring benefit to other related tasks (*e.g.* aesthetic assessment [2, 14], memorability estimation [5, 31], and stylized image captioning [3, 9]), as well as potential applications (*e.g.* opinion mining [20, 32], intelligent advertising [13, 24], and mental disease treatment [15, 34]).

Most of the existing work often regard VEA as a single-label classification task [29, 36, 38, 42, 47], assuming that each image only evokes a dominant emotion. However, these attempts over-simplified the complexity of human emotions and neglected the ambiguity and subjectivity lies in them. In reality, different people may experience different emotions towards one image (*i.e.*, subjectivity), and even an individual may have diverse emotions towards one image (*i.e.*, ambiguity). *Label Distribution Learning (LDL)* is proposed to deal with the problem when an instance is covered by a certain number of labels with different description degrees [7]. Thus, it is more reasonable to address VEA in an LDL paradigm rather than a single-label classification
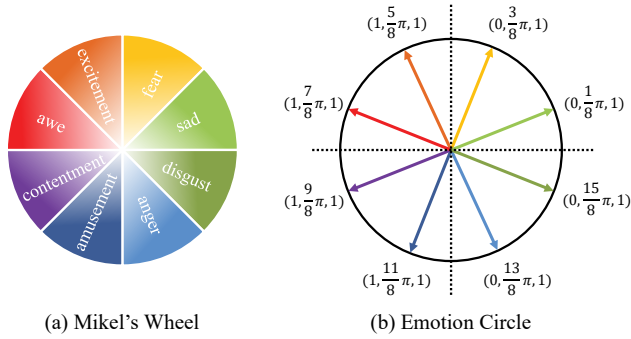
---

*Corresponding author

Figure 2. Mikel's Wheel from psychological model (a), and the proposed Emotion Circle (b) with eight basic emotion vectors evenly distributed in accordance with Mikel's Wheel.

task, as shown in Fig. 1. Various methods have been proposed to deal with visual emotion distribution learning so far, including the earlier traditional algorithms [7, 39, 43] and the recent deep learning ones [11, 26, 35, 37, 39]. Most of the aforementioned methods simply implement general LDL algorithms for VEA. However, unlike other LDL tasks, there exist intrinsic relationships between distinct emotion labels, which can be viewed as useful prior knowledge of this task.

The study of human emotions is not only limited to computer vision field, but also being heated discussed in psychology [17, 33], biology [22, 28], as well as sociology [12, 30]. Psychologists developed various emotion models to illustrate the intrinsic relationships among emotions, including the well-known Plutchik's Wheel [27] and Mikel's Wheel [23, 45]. Besides, it has been demonstrated in psychology that people experience eight basic emotions, which can be expressed at different intensities and can be combined to form any emotional state [27].

Inspired by the above studies, we propose a well-grounded circular-structured representation for visual emotion distribution learning, aiming to effectively utilize the intrinsic relationships between emotions and unique characteristics within them. To be specific, we construct an *Emotion Circle* to unify any emotional state within it, including both basic emotions and the compound ones. On the proposed Emotion Circle, each emotional state can be well-presented as an emotion vector with three attributes (*i.e.*, *emotion polarity*, *emotion type* and *emotion intensity*) and two properties, namely *similarity* and *additivity*. As shown in Fig. 2, basic emotions are defined with a set of unit vectors evenly-distributed on the Emotion Circle (b), corresponding to the circular structure of the eight basic emotions (*i.e.*, amusement, awe, contentment, excitement, anger, disgust, fear, sad) in Mikel's Wheel (a) [23, 45]. In addition to the above basic emotions, there also exist complex emotional states in reality (*e.g.*, emotion distributions). Therefore, considering that basic emotions have intensities and can be combined to form any emotional state [27], we

propose a systematic approach to map any emotion distribution to a compound emotion vector on the Emotion Circle. In detail, each emotion distribution is first projected on basic emotion vectors with different emotion intensities according to their description degrees. Weighted basic emotion vectors are then combined to form a compound emotion vector, which can be regarded as the specific circular-structured representation of a given emotion distribution.

Most visual emotion distribution learning methods [11, 37, 39] simply leverage the *Kullback-Leibler (KL) loss* [18] to directly measure the differences between labeled emotion distributions and the predicted ones. However, rather than a set of uncorrelated labels, emotions are closely related to each other and circularly distributed according to psychological models. To exploit such prior knowledge, we propose a novel *Progressive Circular (PC) loss* to learn the dissimilarities between the labeled emotion vector and the predicted one on the Emotion Circle in a coarse-to-fine manner. In detail, We first construct polar loss to penalize the difference between the predicted polarity and the labeled one, which can be viewed as a coarse constraint towards a specific emotional state. After divide emotions into two polarities, we build up a more fine-grained constraint on emotion type by calculating the distance between them. Since emotion intensity is regarded as a crucial factor when describing a specific emotional state [27], we further leverage it as the confidence degree to constrain the above two losses. By implementing both the KL loss and the proposed PC loss, the learning process of emotion distribution is not only optimized through its conventional mechanism, but also further boosted in a novel emotion-specific circular-structured manner.

Our contributions can be summarized as follows:

- We propose a well-grounded circular-structured representation to learn visual emotion distribution by utilizing the intrinsic relationships between emotions, which consistently outperforms the state-of-the-art methods on several emotion distribution datasets. To the best of our knowledge, it is the first time to systematically exploit emotion relationships as prior knowledge for visual emotion distribution learning.

- We construct an Emotion Circle to unify any emotional state within it, where each emotion distribution is represented as a compound emotion vector with three attributes as well as two properties according to psychological models.

- We design a novel Progressive Circular loss to penalize the dissimilarities between labeled emotion vectors and the predicted ones on the Emotion Circle from coarse to fine, which further boosts the visual emotion distribution learning process in an emotion-specific circular-structured manner.
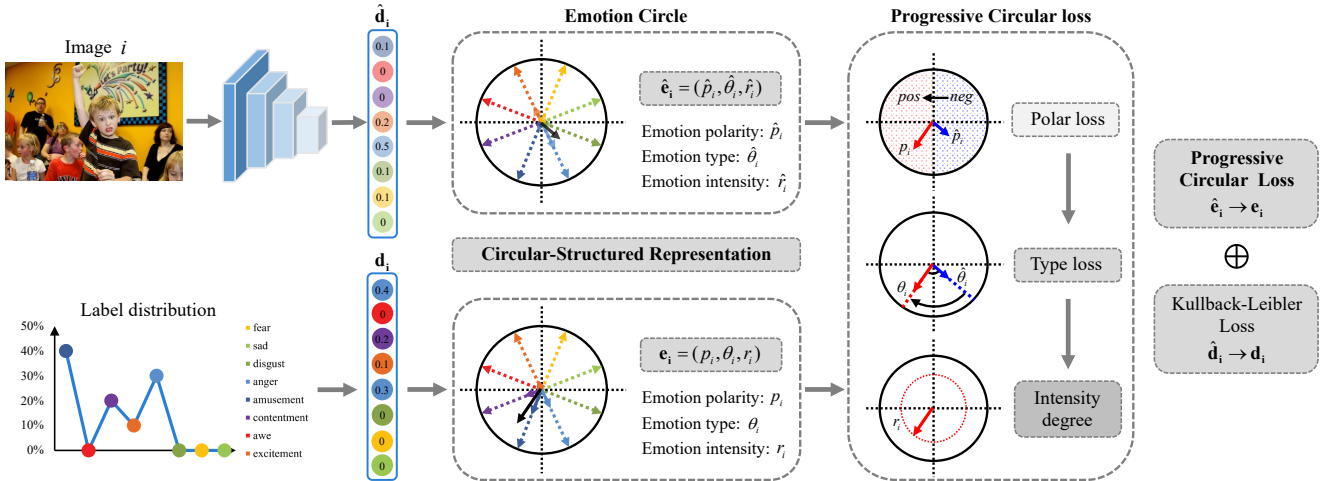
Figure 3. Framework of the proposed circular-structured representation. On the proposed Emotion Circle, both the predicted emotion distribution and the labeled one are represented with compound emotion vectors through a systematic approach. We then propose the Progressive Circular loss in a coarse-to-fine manner, which is further exploited to train the network together with Kullback-Leibler loss.

2. Related Work

2.1. Visual Emotion Analysis

Researchers have been devoted to visual emotion analysis (VEA) for more than two decades [19], during which approaches vary from the early traditional ones to the recent deep learning ones. Earlier works in VEA mainly focused on designing hand-crafted features to mine emotions from affective images [1, 21, 44, 46]. Inspired by psychology and art theory, Machajdik *et al.* [21] extracted rich hand-crafted features including color, texture, composition, and content. Zhao *et al.* [46] extracted features from low-level elements-of-art, mid-level principles-of-art, to high-level semantics in a multi-graph learning framework. Although hand-crafted features have been proven to be effective on several small-scale datasets, they are still limited to cover all the important factors in visual emotion. Recently, researchers in VEA have adopted Convolutional Neural Network (CNN) to predict emotions and have achieved gratifying results [29, 36, 38, 40, 41, 42]. A multi-level deep representation network (MldrNet) was constructed by Rao *et al.* [29] to extract emotional features from image semantics, aesthetics, and low-level features simultaneously. Aiming to focus on local regions instead of the holistic one, Yang *et al.* [38] constructed a local branch to discover affective regions (AR) by implementing the off-the-shelf detection tools. A weakly supervised coupled network (WSCNet) [36] was further proposed by Yang *et al.* to discover emotion regions as well as to predict visual emotions in an end-to-end manner. However, these methods simply regard VEA as a single-label classification task, which neglects the ambiguity and subjectivity lies in human emotions. To be specific, different people may evoke different emotions towards one image (*i.e.*, subjectivity) and even an individual

may experience multiple emotions towards one image (*i.e.*, ambiguity). Thus, rather than a single-label classification task, it is more reasonable to consider VEA in a Label Distribution Learning [27] paradigm.

2.2. Label Distribution Learning

Label distribution learning (LDL) is proposed by Geng *et al.* [7] to address the problem when an instance is covered by a certain number of labels with different description degrees, which is a more general learning framework covering both single-label and multi-label learning tasks. Traditional algorithms in LDL can be roughly divided into three strategies, *i.e.*, problem transfer (PT), algorithm adaption (AA), and specialized algorithms (SA) [7]. With the help of deep networks, deep label distribution learning (DLDL) is proposed by Gao *et al.* [6] to effectively prevent the network from over-fitting by utilizing the label ambiguity in both feature learning and classifier learning. Consequently, LDL was then introduced to VEA to deal with subjectivity and ambiguity lies in it [11, 26, 35, 37, 39, 43]. Peng *et al.* [26] proposed convolutional neural network regressions (CNNR) to address VEA in LDL for the first time. Subsequently, Yang *et al.* [37] proposed a joint network (JCDL) to learn visual emotion from distribution and classification simultaneously, by optimizing both softmax loss and Kullback-Leibler (KL) loss. Most of the aforementioned methods simply employ general LDL mechanisms and consequently ignore the intrinsic relationships between emotions, which can be regarded as prior knowledge for visual emotion distribution learning. Motivated by psychological theories [23, 27, 45], we propose a circular-structured representation to utilize the intrinsic relationships between emotions and unique characteristics within it.
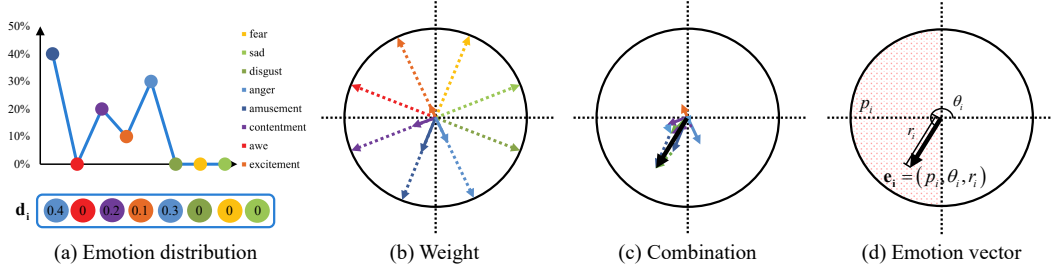
Figure 4. Mapping from the emotion distribution (a) to the compound emotion vector (d) on the Emotion Circle. We first weigh eight basic emotions with different description degrees (b) and then combine them to form a compound emotion vector through vector addition operations (c). The final emotion vector can be viewed as a specific circular-structured representation of a given emotion distribution.

3. Methodology

3.1. Emotion Circle

Unlike other label distribution learning tasks, emotion labels are closely related to each other with circular structure and unique characteristics based on psychological models [23, 27, 45]. Inspired by this, aiming at learning emotions in a more specific and reasonable way, we construct an Emotion Circle to unify any emotional states in it. On the proposed Emotion Circle, each emotional state is represented with an emotion vector $\mathbf{e_i}$, which is described as

$$\mathbf{e_i} = (p_i, \theta_i, r_i), \qquad (1)$$

where p_i, θ_i, r_i denotes the emotion polarity, emotion type and emotion intensity respectively. We give detailed definitions of the above three emotion attributes as follows and further introduce two properties for emotion vectors according to psychological theories.

- **Emotion Polarity** (p_i): In addition to its given emotion label (*i.e.*, amusement, awe, contentment, excitement, anger, disgust, fear, sad), each emotion is also naturally grouped into a specific emotion polarity (*i.e.*, positive, negative). Specifically, amusement, awe, contentment, excitement belong to positive emotions while anger, disgust, fear, sad are negative ones. Hence, we divide the Emotion Circle to half positive and half negative, as given in Eq. 2, in accordance with the polar structure on the Mikel's Wheel [23, 45]:

$$p_i = \begin{cases} 0, & \theta_i \in \left[0, \frac{1}{2}\pi\right) \cup \left[\frac{3}{2}\pi, 2\pi\right), \\ 1, & \theta_i \in \left[\frac{1}{2}\pi, \frac{3}{2}\pi\right). \end{cases} \qquad (2)$$

- **Emotion Type** (θ_i): We define emotion type with the polar angle $\theta_i \in [0, 2\pi]$, in order to preserve the circular-distributed emotions on the Mikel's Wheel. There are basic emotions and compound emotions in reality [27], which both can be well-represented on the Emotion Circle. In Fig. 2(b), we first set a series of evenly-distributed unit vectors on the Emotion Circle

to represent eight basic emotions, denoted as

$$\theta^j = \frac{2j-1}{8}\pi, j \in [1, C], \qquad (3)$$

where C denotes the number of emotion categories in psychological models. Besides, there also exist compound emotion types, which are distributed in the blank space between these basic vectors.

- **Emotion Intensity** (r_i): As mentioned in a psychological literature [27], "Each emotion can exist in varying degrees of intensity." Thus, polar diameter $r_i \in [0, 1]$ is introduced to describe the intensity of a specific emotion type θ_i, where $r_i = 1$ indicates the strongest degree and $r_i = 0$ the weakest. To be specific, the emotion intensity of each basic emotion is set as

$$r^j = 1, j \in [1, C], \qquad (4)$$

indicating that only a single emotion described the specific emotional state with all its weight.

- **Similarity**: The similarity between different emotions are measured with the distance between their polar angles, *i.e.*, image i_1 and image i_2 share the same emotion type if and only if $\theta_{i_1} = \theta_{i_2}$. As mentioned in a psychological literature [27], "since a circle combines the concepts of degree of similarity (nearness) and degree of opposition". The larger the distance between two polar angles, the greater the dissimilarities between two emotion types.

- **Additivity**: According to psychological theories [27], basic emotion vectors can be intensified and combined to produce any complex emotional states. Thus, each compound emotion can be defined as a weighted combination of basic emotions, which can be calculated through vector addition operations.

Based on the aforementioned attributes and properties, we develop a systematic approach to map an emotion distribution to a compound emotion vector on the Emotion Circle, as shown in Algorithm 3.1. Besides the strict arithmetic procedures, we also vividly illustrate the mapping process in Fig. 4 for better comprehension. In general, each

Algorithm 1 Circular-structured emotion representation

Input: Emotion distribution: $\mathbf{d_i} = \left[d_i^1, ... d_i^C \right]$
Output: Compound emotion vector: $\mathbf{e_i} = (p_i, \theta_i, r_i)$

1: **for** $i = 1; i < N; i + + $ **do**
2:     **for** $j = 1; j < C; j + + $ **do**
3:         Initialize basic emotion vectors,
4:         $\mathbf{e^j} = (p^j, \theta^j, r^j);$
5:         Weight basic emotion vectors,
6:         $\mathbf{e_i^j} = d_i^j \times \mathbf{e^j} \triangleq \left(p_i^j, \theta_i^j, r_i^j \right);$
7:         Polar coordinate to Cartesian coordinate,
8:         $\begin{cases} x_i^j = r_i^j \cos \theta_i^j, \\ y_i^j = r_i^j \sin \theta_i^j; \end{cases}$
9:     Combination of weighted basic emotion vectors,
10:    $x_i = \sum_{j=1}^C x_i^j, \;\; y_i = \sum_{j=1}^C y_i^j;$
11:    Cartesian coordinate to Polar coordinate,
12:    $\begin{cases} r_i = \sqrt{x_i^2 + y_i^2}, \\ \theta_i = \arctan(y_i/x_i); \end{cases}$
13:    **if** $\theta_i \in \left[0, \frac{1}{2}\pi\right) \cup \left[\frac{3}{2}\pi, 2\pi\right)$ **then**
14:        $p_i = 0,$
15:    **else**
16:        $p_i = 1;$
17:    Compound emotion vector: $\mathbf{e_i} = (p_i, \theta_i, r_i);$
18: **return** $\mathbf{e_i}$

emotion distribution is first projected on basic emotion vectors with different emotion intensities according to their description degrees. Weighted basic emotion vectors are then combined, based on the intrinsic circular structure between emotions, to form a compound emotion vector, which can be regarded as the specific circular-structured representation of a given emotion distribution.

3.2. Progressive Circular Loss

Most of the previous methods simply implement the Kullback-Leibler (KL) [18] loss for visual emotion distribution learning, which measure the information loss caused by the inconsistency between the predicted distribution and the labeled one:

$$\mathcal{L}_{KL} = -\frac{1}{N} \sum_{i=1}^N \sum_{j=1}^C \mathbf{d_i}(j) \ln \hat{\mathbf{d_i}}(j), \qquad (5)$$

$$\hat{\mathbf{d_i}}(j|\mathbf{f}_i, \mathbf{W}) = \frac{\exp(\mathbf{w}_{i,j}\mathbf{f}_i)}{\sum_{j=1}^C \exp(\mathbf{w}_{i,j}\mathbf{f}_i)}, \qquad (6)$$

where $\mathbf{d_i}$ denotes the labeled emotion distribution from datasets and $\hat{\mathbf{d_i}}$ represents the predicted one. N denotes the number of images in a specific dataset and C represents the involved emotion categories.

However, rather than a set of uncorrelated labels, emotions are intrinsically distributed in a circular structure in

psychological models [23, 45]. In order to effectively exploit such prior knowledge, we propose a Progressive Circular (PC) loss to learn the emotion distribution from coarse to fine. The proposed PC loss, conducted on the Emotion Circle described in Sec. 3.1, is designed to penalize the difference between two emotion vectors, *i.e.*, the labeled one $\mathbf{e_i} = (p_i, \theta_i, r_i)$ and the predicted one $\hat{\mathbf{e_i}} = (\hat{p}_i, \hat{\theta}_i, \hat{r}_i)$. To be specific, we progressively establish constraints on three attributes of emotion vectors, *i.e.*, emotion polarity (p_i), emotion type (θ_i) and emotion intensity (r_i). Since polarity is the coarse attribute of an emotion, we first devise polar loss to measure the differences between emotion polarities, by implementing the Mean Square Error (MSE) loss:

$$\mathcal{L}_p = \frac{1}{N} \sum_{i=1}^N (p_i - \hat{p}_i)^2, \qquad (7)$$

where p_i denotes the labeled emotion polarity and $\hat{p}_i$ represents the predicted one. Eq. 7 ensures the correctness in emotion polarity prediction, which is the first goal towards accurate emotion prediction. As mentioned in Sec. 3.1, distance between polar angles can measure the similarities between different emotion types. Thus, after divide emotions into two polarities, we build up a more fine-grained constraint on emotion type, denoted as type loss:

$$\mathcal{L}_t = \frac{1}{N} \sum_{i=1}^N (\theta_i - \hat{\theta}_i)^2. \qquad (8)$$

In Eq. 8, the closer the two polar angles are, the more similarity lies in their emotional states. However, it is insufficient to merely take emotion type into account, as emotion intensity is also considered as a crucial factor towards a specific emotional state [27]. Suppose there are two images with the same emotion type, *i.e.*, $\theta_{i_1} = \theta_{i_2}$, and quite different emotion intensities, *i.e.*, $r_{i_1} = 1$, $r_{i_2} = 0.01$, it is really hard to group them into the same emotional state. Therefore, serving as the confidence degree for both emotion type θ_i and emotion polarity p_i, we further add emotion intensity r_i to the proposed loss function for a precise and detailed constraint for visual emotion distribution learning:

$$\mathcal{L}_{PC} = \frac{1}{N} \sum_{i=1}^N r_i \left((p_i - \hat{p}_i)^2 + (\theta_i - \hat{\theta}_i)^2 \right). \qquad (9)$$

Based on the Emotion Circle, our PC loss is eventually constructed with three constraints in a coarse-to-fine manner in Eq. 9. Our loss function is integrated with both KL loss and PC loss in a weighted combination:

$$\mathcal{L} = (1 - \mu)\mathcal{L}_{KL} + \mu\mathcal{L}_{PC}, \qquad (10)$$

where μ is a hyper-parameter balancing the importance between the two losses and is further ablated in Sec. 4.4.2. So

Table 1. Comparison with the state-of-the-art methods on Flickr_LDL dataset.

| Measures | PT | | AA | | SA | | | CNN-based | | | | | | |
	PT-Bayes	PT-SVM	AA-kNN	AA-BP	SA-IIS	SA-BFGS	SA-CPNN	CNNR	DLDL	ACPNN	JCDL	SSDL	E-GCN	Ours
Chebyshev ↓	0.44(13)	0.55(14)	0.28(8)	0.36(11)	0.31(10)	0.37(12)	0.30(9)	0.25(5)	0.25(5)	0.25(5)	0.24(4)	0.23(2)	0.23(2)	**0.21(1)**
Clark ↓	0.89(14)	0.87(13)	**0.57(1)**	0.82(8)	0.82(8)	0.86(12)	0.82(8)	0.84(11)	0.78(5)	0.77(2)	0.77(2)	0.78(5)	0.78(5)	0.77(2)
Canberra ↓	0.85(14)	0.83(13)	**0.41(1)**	0.75(10)	0.75(10)	0.82(12)	0.74(9)	0.73(8)	0.70(7)	0.70(5)	0.70(5)	0.69(3)	0.69(3)	0.68(2)
KL ↓	1.88(13)	1.69(12)	3.28(14)	0.82(10)	0.66(7)	1.06(11)	0.71(9)	0.70(8)	0.54(5)	0.62(6)	0.53(4)	0.46(3)	0.44(2)	**0.41(1)**
Cosine ↑	0.63(13)	0.32(14)	0.79(7)	0.72(9)	0.78(8)	0.70(11)	0.70(11)	0.72(9)	0.81(5)	0.80(6)	0.82(4)	0.85(3)	0.86(2)	**0.87(1)**
Intersection ↑	0.49(13)	0.29(14)	0.64(5)	0.53(12)	0.60(9)	0.56(11)	0.60(9)	0.62(7)	0.64(5)	0.62(7)	0.65(4)	0.68(3)	0.69(2)	**0.71(1)**
Average Rank ↓	13.3(13)	13.3(13)	6(7)	10(11)	8.7(9)	11.5(12)	9.2(10)	8(8)	5.3(6)	5.2(5)	3.8(4)	3.2(3)	2.7(2)	**1.3(1)**
Accuracy ↑	0.47(13)	0.37(14)	0.61(5)	0.52(11)	0.58(9)	0.50(12)	0.58(9)	0.61(5)	0.61(5)	60.0(8)	0.64(4)	0.70(2)	0.69(3)	**0.72(1)**

Table 2. Comparison with the state-of-the-art methods on Twitter_LDL dataset.

| Measures | PT | | AA | | SA | | | CNN-based | | | | | | |
	PT-Bayes	PT-SVM	AA-kNN	AA-BP	SA-IIS	SA-BFGS	SA-CPNN	CNNR	DLDL	ACPNN	JCDL	SSDL	E-GCN	Ours
Chebyshev ↓	0.53(13)	0.63(14)	0.28(7)	0.37(11)	0.28(7)	0.37(11)	0.36(10)	0.28(7)	0.26(5)	0.27(6)	0.25(3)	0.25(3)	0.24(2)	**0.22(1)**
Clark ↓	0.85(7)	0.91(14)	**0.58(1)**	0.89(12)	0.86(11)	0.89(12)	0.85(7)	0.84(3)	0.84(3)	0.85(7)	0.83(2)	0.84(3)	0.85(7)	0.84(3)
Canberra ↓	0.77(6)	0.88(14)	**0.41(1)**	0.84(12)	0.79(11)	0.84(12)	0.78(8)	0.76(2)	0.77(6)	0.78(8)	0.76(2)	0.76(2)	0.78(8)	0.76(2)
KL ↓	1.31(12)	1.65(13)	3.89(14)	1.19(10)	0.64(7)	1.19(10)	0.85(9)	0.67(7)	0.54(6)	0.58(6)	0.53(4)	0.51(3)	0.46(2)	**0.44(1)**
Cosine ↑	0.53(13)	0.25(14)	0.82(7)	0.71(11)	0.82(7)	0.71(11)	0.75(10)	0.82(7)	0.83(6)	0.84(5)	0.85(4)	0.86(3)	0.87(2)	**0.89(1)**
Intersection ↑	0.40(13)	0.21(14)	0.66(5)	0.59(9)	0.63(8)	0.57(11)	0.56(12)	0.58(10)	0.65(6)	0.64(7)	0.68(4)	0.69(3)	0.70(2)	**0.72(1)**
Average Rank ↓	10.7(12)	13.8(14)	5.8(6)	10.8(11)	8.5(9)	11.2(13)	9.3(10)	6(7)	5.2(5)	6.5(8)	3.2(3)	2.8(2)	3.8(4)	**1.5(1)**
Accuracy ↑	0.45(13)	0.40(14)	0.73(7)	0.72(9)	0.70(10)	0.57(12)	0.70(10)	0.74(5)	0.73(7)	0.74(5)	0.76(3)	0.77(2)	0.76(3)	**0.78(1)**

far, the emotion distribution is not only learned in a conventional mechanism, but further gains a performance boost in an emotion-specific and circular-structured manner.

4. Experimental Results

4.1. Datasets

We evaluate our method on three public visual emotion distribution datasets, including Flickr_LDL, Twitter_LDL [39] and Abstract Paintings [21]. Built on Mikel's eight emotion space, there are 11,150 images in Flickr_LDL and 10,045 images in Twitter_LDL. Eleven viewers are hired to label Flickr_LDL and eight viewers are hired to label Twitter_LDL, where the detailed votes from all the workers are integrated to generate the ground truth label distribution for each image. The Abstract Paintings dataset is also labeled with Mikel's eight emotions, which consists only of combinations of color and texture without any recognizable objects and contains 280 images in total.

4.2. Implementation Details

In the experiment, our backbone network is built on ResNet-50 [10] following the same setting as previous methods [11], which is pre-trained on a large-scale visual recognition dataset, ImageNet [4]. Specifically, the output dimension of the last fully connected layer is changed to emotion numbers according to the datasets. Following the same setting in [39], Flickr_LDL, Twitter_LDL and Abstract Paintings datasets are randomly split into training set (80%) and testing set (20%). For training/testing sets, after resizing each image to 480 on its shorter side, we then crop it to 448×448 randomly followed by a horizontal flip [10].

The whole network is trained by the adaptive optimizer Adam [16] in an end-to-end manner with KL loss and the proposed PC loss. With a weight decay of 5e-5, the learning rate of Adam starts from 1e-5 and divided by 10 every 10 epochs, and the total epoch number is set to 50. Our framework is implemented using PyTorch [25] and our experiments are performed on an NVIDIA GTX 1080Ti GPU.

4.3. Comparison with the State-of-the-art Methods

To evaluate the effectiveness of the proposed circular-structured representation, we conduct extensive experiments compared with the state-of-the-art methods on three public visual emotion distribution datasets, including Flickr_LDL, Twitter_LDL and Abstract Paintings, as shown in TABLE 1, TABLE 2 and TABLE 3 respectively. In general, the state-of-the-art methods can be divided into four types: PT, AA, SA and CNN-based.

- **Problem Transformation (PT)**: Based on the representative algorithms Bayes classifier and SVM, PT-Bayes and PT-SVM are designed to transfer the LDL problem into a single-label learning (SLL) one [7]. Since these methods roughly turn a complex LDL task into a simple SLL one, performance drops may exist when measuring the differences between distributions.
- **Algorithm Adaptation (AA)**: The existing machine learning algorithms k-NN and BP neural network are extended to deal with label distributions, which are denoted by AA-kNN and AA-BP respectively [7]. In TABLE 1 and TABLE 2, AA-kNN achieves insurmountable results in Clark distance and Canberra metric, owing to its superiority in dealing with overlapping samples in visual emotion distributions.

Table 3. Comparison with the state-of-the-art methods on Abstract Paintings dataset.

| Measures	PT		AA		SA		CNN-based	
	PT-Bayes	PT-SVM	AA-kNN	AA-BP	SA-IIS	SA-BFGS	ACPNN	Ours
Chebyshev ↓	0.360(7)	0.298(6)	0.245(3)	0.297(5)	0.296(4)	0.472(8)	0.234(2)	**0.226(1)**
Clark ↓	0.674(7)	0.632(4)	0.621(2)	0.641(5)	0.660(6)	0.834(8)	0.625(3)	**0.562(1)**
Canberra ↓	0.594(7)	0.537(4)	0.513(2)	0.544(6)	0.564(5)	0.781(8)	0.522(3)	**0.456(1)**
KL ↓	3.268(8)	0.708(5)	0.515(3)	0.782(6)	0.644(4)	2.282(7)	0.513(2)	**0.441(1)**
Cosine ↑	0.653(5)	0.643(6)	0.753(3)	0.636(7)	0.692(4)	0.573(8)	0.763(2)	**0.773(1)**
Intersection ↑	0.518(7)	0.539(6)	0.608(3)	0.540(5)	0.577(4)	0.417(8)	0.618(2)	**0.654(1)**
Average Rank ↓	6.83(7)	5.17(6)	2.68(3)	4.83(5)	3.83(4)	7.83(8)	2.33(2)	**1(1)**

Table 4. Ablation study of loss function on Flickr_LDL dataset.

Measures	$\mathcal{L}_{KL}$	$\mathcal{L}_{KL}+\mathcal{L}_p$	$\mathcal{L}_{KL}+\mathcal{L}_t$	$\mathcal{L}_{KL}+\mathcal{L}_p+\mathcal{L}_t$	$\mathcal{L}_{KL}+\mathcal{L}_{PC}$
Chebyshev ↓	0.239	0.225	0.222	0.218	**0.213**
Clark ↓	0.783	0.779	0.779	0.775	**0.774**
Canberra ↓	0.697	0.689	0.687	**0.682**	0.685
KL ↓	0.435	0.441	0.420	0.414	**0.408**
Cosine ↑	0.843	0.862	0.869	0.870	**0.874**
Intersection ↑	0.678	0.693	0.705	0.703	**0.709**
Accuracy ↑	0.669	0.695	0.700	0.718	**0.721**

Table 5. Ablation study of loss function on Twitter_LDL dataset.

Measures	$\mathcal{L}_{KL}$	$\mathcal{L}_{KL}+\mathcal{L}_p$	$\mathcal{L}_{KL}+\mathcal{L}_t$	$\mathcal{L}_{KL}+\mathcal{L}_p+\mathcal{L}_t$	$\mathcal{L}_{KL}+\mathcal{L}_{PC}$
Chebyshev ↓	0.259	0.240	0.233	0.230	**0.224**
Clark ↓	0.861	0.851	0.848	0.846	**0.842**
Canberra ↓	0.797	0.778	0.775	0.772	**0.764**
KL ↓	0.464	0.476	0.455	0.450	**0.439**
Cosine ↑	0.848	0.870	0.878	0.882	**0.886**
Intersection ↑	0.686	0.706	0.703	0.713	**0.717**
Accuracy ↑	0.744	0.764	0.770	0.779	**0.781**

- **Specialized Algorithm (SA)**: Specialized algorithms are designed by directly matching the characteristics of LDL, including SA-IIS, SA-BFGS, SA-CPNN [7, 8]. By implementing a similar strategy to Improved Iterative Scaling (IIS), SA-IIS assumes the parametric model to be the maximum entropy mode [7, 8]. However, IIS often performs worse compared with other optimization algorithms such as conjugate gradient and quasi-Newton methods. Thus, SA-BFGS is further developed with an effective quasi-Newton method named Broyden-Fletcher-Goldfarb-Shanno for LDL [7]. SA-CPNN is proposed based on a three-layer conditional probability neural network [8]. Compared with the above PT and AA methods, SA has achieved improved results for their specially designed features.

- **CNN-based methods (CNN-based)**: Benefiting from its powerful representation ability, CNN-based methods gain a significant performance boost compared with those traditional ones. Specifically, CNNR [26] is proposed to treat VEA in a label distribution paradigm for the first time, which achieved a great performance with an end-to-end network. DLDL [6] replaces the Euclidean loss with KL loss to well describe the differences between two distributions. In order to learn visual emotion distribution and classification in a joint manner, JCDL [37] further boosts the performance by optimizing both KL loss and softmax loss.
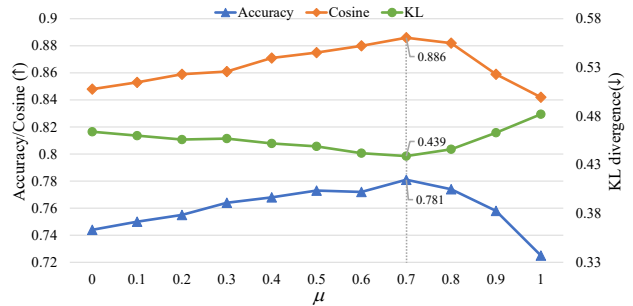
Figure 5. Effect of μ for combined loss on Twitter_LDL dataset. Note that $\mu = 1$ suggests only using PC loss while $\mu = 0$ means implementing KL loss alone.

Following the same setting as the previous work [7, 11, 35, 37, 39], we evaluate the performance of visual emotion distribution learning task with six commonly-used measurements, *i.e.*, Chebyshev distance (↓), Clark distance (↓), Canberra metric (↓), Kullback-Leibler divergence (↓), cosine coefficient (↑), and intersection similarity (↑). Among these measurements, the first four are distance measures and the last two are similarity measures, where ↓ suggests the lower the better and ↑ the higher the better. As KL divergence is not well defined with zero value, we use a small value $\varepsilon = 10^{-10}$ to approximate it. Besides, since the maximum values of Clark distance and Canberra metric are determined by the number of emotions, we divided Clark distance by the square root of number of emotions and divided Canberra metric by the number of emotions for standardized comparisons. In addition to the above six measurements, we further introduce top-1 accuracy as another evaluation metric, which ensures the prediction results of the dominant emotions in the distributions. From the above analysis, it is obvious that the proposed method consistently outperforms the state-of-the-art methods on three widely-used datasets, owing to the effectiveness in circular-structured representation for visual emotion distribution learning.

4.4. Ablation Study

4.4.1 Effectiveness of the PC Loss

In TABLE 4 and TABLE 5, we conduct ablation study on the proposed PC loss with two large-scale datasets, aiming to verify the effectiveness of each proposed constraint (*i.e.*, polar loss, type loss and emotion intensity). By adopting
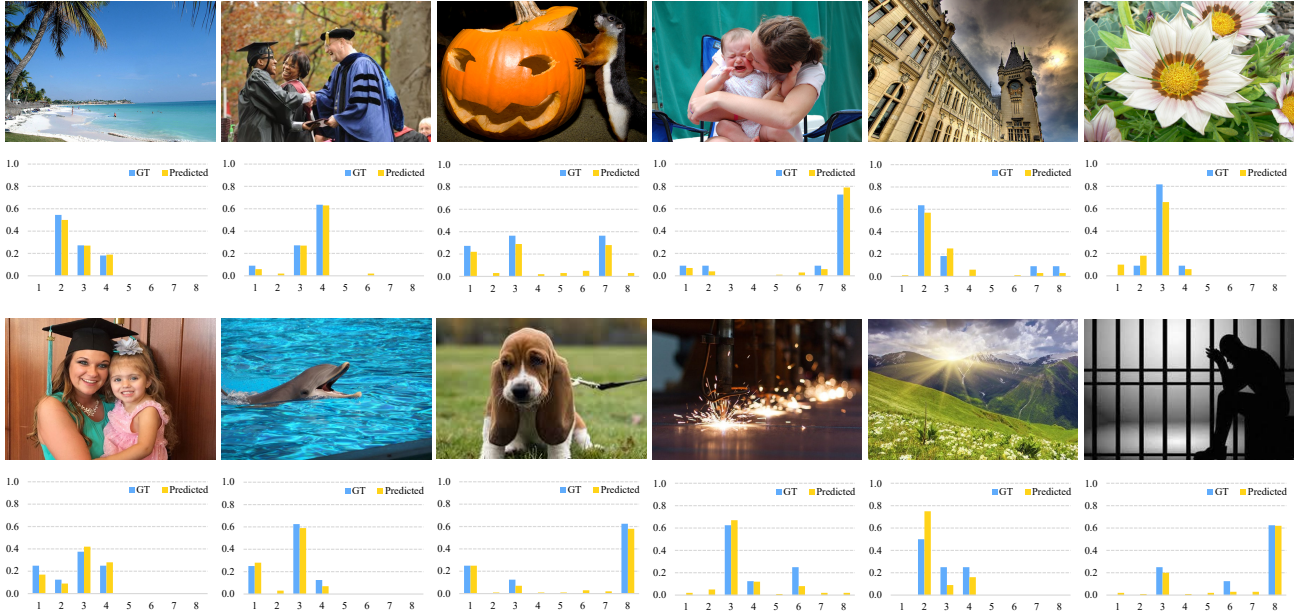
Figure 6. Visualization of the predicted emotion distributions (predicted) and the ground-truth (GT) ones, where images in the first line come from Flickr_LDL dataset and second line the Twitter_LDL. Each number on the horizontal axis corresponds to an emotion category.

KL loss alone, we first evaluate the baseline of our method with six measurements and top-1 accuracy. Polarity loss and type loss are then separately and jointly added to KL loss, where both bring significant performance boosts as emotion polarity and emotion type serve as the basic and decisive attributes in visual emotion distribution learning. For a more fine-grained description, emotion intensity further improves all the measurements and gains the optimal result eventually. From the above analysis, we can conclude that each constraint in PC loss is indispensable, jointly and progressively contributing to the final result.

4.4.2 Hyper-Parameter Analysis

As μ controls the relative importance between the proposed PC loss and KL loss, we conduct experiments to validate the choice of $\mu = 0.7$ in Eq. 10, as shown in Fig. 5. The greater the value of μ, the more importance lies in the proposed PC loss. Based on the Twitter_LDL dataset, we implement three measurements, namely KL divergence, Cosine coefficient and Accuracy, to demonstrate how μ influences the performance of the proposed method. We find that all the three measurements constantly grows as μ varies from 0 to 0.7 and drops after $\mu = 0.7$, which suggests that a combination of PC loss and KL loss achieves the best performance. As KL loss solves the problem of general label distribution learning while PC loss considers emotion-specific circular structure as prior knowledge, each loss encounters performance drop when acting alone, which further suggests that both losses are essential and complementary in visual emotion distribution learning.

4.5. Visualization

We further visualize the predicted emotion distributions (predicted) and the ground-truths (GT) on both Flickr_LDL and Twitter_LDL datasets in Fig. 6. It is obvious that the proposed method restores the original emotion distribution to a large extent on both emotion polarity, emotion type and emotion intensity. Specifically, we can infer from the visualized results that once an emotion distribution only involves a single polarity, the prediction is more accurate with the help of the polar loss. When encounters complex emotional state, i.e., an emotional state is made up of different polarized emotions, our proposed method can still achieve relatively good results, owing to the effectiveness of the proposed type loss and emotion intensity.

5. Conclusion

In this paper, we have proposed a circular-structured representation for visual emotion distribution learning by exploiting the intrinsic relationships between emotions based on psychological models. We first constructed the Emotion Circle to present any emotional state with emotion vectors and then designed a Progressive Circular (PC) loss to constraint emotion vectors in a coarse-to-fine manner. Extensive experiments and comparisons have shown that the proposed method consistently outperforms the state-of-the-art methods on three visual emotion distribution datasets.

References

[1] Damian Borth, Rongrong Ji, Tao Chen, Thomas Breuel, and Shih-Fu Chang. Large-scale visual sentiment ontology and detectors using adjective noun pairs. In *ACMMM*, pages 223–232, 2013. 3

[2] Qiuyu Chen, Wei Zhang, Ning Zhou, Peng Lei, Yi Xu, Yu Zheng, and Jianping Fan. Adaptive fractional dilated convolution network for image aesthetics assessment. In *CVPR*, pages 14114–14123, 2020. 1

[3] Tianlang Chen, Zhongping Zhang, Quanzeng You, Chen Fang, Zhaowen Wang, Hailin Jin, and Jiebo Luo. "factual"or"emotional": Stylized image captioning with adaptive learning and attention. In *ECCV*, pages 519–535, 2018. 1

[4] Jia Deng, Wei Dong, Richard Socher, Li-Jia Li, Kai Li, and Li Fei-Fei. Imagenet: A large-scale hierarchical image database. In *CVPR*, pages 248–255, 2009. 6

[5] Jiri Fajtl, Vasileios Argyriou, Dorothy Monekosso, and Paolo Remagnino. Amnet: Memorability estimation with attention. In *CVPR*, pages 6363–6372, 2018. 1

[6] Bin-Bin Gao, Chao Xing, Chen-Wei Xie, Jianxin Wu, and Xin Geng. Deep label distribution learning with label ambiguity. *IEEE Transactions on Image Processing*, 26(6):2825–2838, 2017. 3, 7

[7] Xin Geng. Label distribution learning. *IEEE Transactions on Knowledge and Data Engineering*, 28(7):1734–1748, 2016. 1, 2, 3, 6, 7

[8] Xin Geng, Chao Yin, and Zhi-Hua Zhou. Facial age estimation by learning from label distributions. *IEEE transactions on pattern analysis and machine intelligence*, 35(10):2401–2412, 2013. 7

[9] Longteng Guo, Jing Liu, Peng Yao, Jiangwei Li, and Hanqing Lu. Mscap: Multi-style image captioning with unpaired stylized text. In *CVPR*, pages 4204–4213, 2019. 1

[10] Kaiming He, Xiangyu Zhang, Shaoqing Ren, and Jian Sun. Deep residual learning for image recognition. In *CVPR*, pages 770–778, 2016. 6

[11] Tao He and Xiaoming Jin. Image emotion distribution learning with graph convolutional networks. In *ICMR*, pages 382–390, 2019. 2, 3, 6, 7

[12] Arlie Russell Hochschild. The sociology of emotion as a way of seeing. *Emotions in social life: Critical themes and contemporary issues*, pages 3–15, 1998. 2

[13] Morris B Holbrook and John O'Shaughnessy. The role of emotion in advertising. *Psychology & Marketing*, 1(2):45–64, 1984. 1

[14] Vlad Hosu, Bastian Goldlucke, and Dietmar Saupe. Effective aesthetics prediction with multi-level spatially pooled features. In *CVPR*, pages 9375–9383, 2019. 1

[15] Ming Jiang and Qi Zhao. Learning visual attention to identify people with autism spectrum disorder. In *ICCV*, pages 3267–3276, 2017. 1

[16] Diederik P Kingma and Jimmy Ba. Adam: A method for stochastic optimization. *arXiv preprint arXiv:1412.6980*, 2014. 6

[17] Sander L Koole. The psychology of emotion regulation: An integrative review. *Cognition and emotion*, 23(1):4–41, 2009. 2

[18] Solomon Kullback and Richard A Leibler. On information and sufficiency. *The annals of mathematical statistics*, 22(1):79–86, 1951. 2, 5

[19] Peter J Lang, Margaret M Bradley, Bruce N Cuthbert, et al. International affective picture system (iaps): Technical manual and affective ratings. *NIMH Center for the Study of Emotion and Attention*, 1:39–58, 1997. 3

[20] Zuhe Li, Yangyu Fan, Bin Jiang, Tao Lei, and Weihua Liu. A survey on sentiment analysis and opinion mining for social multimedia. *Multimedia Tools and Applications*, 78(6):6939–6967, 2019. 1

[21] Jana Machajdik and Allan Hanbury. Affective image classification using features inspired by psychology and art theory. In *ACMMM*, pages 83–92, 2010. 3, 6

[22] Neil McNaughton, N McNaughton, and Colin Mcnaughton. *Biology and emotion*. Cambridge University Press, 1989. 2

[23] Joseph A Mikels, Barbara L Fredrickson, Gregory R Larkin, Casey M Lindberg, Sam J Maglio, and Patricia A Reuter-Lorenz. Emotional category data on images from the international affective picture system. *Behavior research methods*, 37(4):626–630, 2005. 2, 3, 4, 5

[24] Andrew A Mitchell. The effect of verbal and visual components of advertisements on brand attitudes and attitude toward the advertisement. *Journal of Consumer Research*, 13(1):12–24, 1986. 1

[25] Adam Paszke, Sam Gross, Soumith Chintala, Gregory Chanan, Edward Yang, Zachary DeVito, Zeming Lin, Alban Desmaison, Luca Antiga, and Adam Lerer. Automatic differentiation in pytorch. 2017. 6

[26] Kuan-Chuan Peng, Tsuhan Chen, Amir Sadovnik, and Andrew C Gallagher. A mixed bag of emotions: Model, predict, and transfer emotion distributions. In *CVPR*, pages 860–868, 2015. 2, 3, 7

[27] Robert Plutchik. A general psychoevolutionary theory of emotion. In *Theories of emotion*, pages 3–33. Elsevier, 1980. 2, 3, 4, 5

[28] Robert Plutchik. *The psychology and biology of emotion*. HarperCollins College Publishers, 1994. 2

[29] Tianrong Rao, Xiaoxu Li, and Min Xu. Learning multi-level deep representations for image emotion classification. *Neural Processing Letters*, pages 1–19, 2016. 1, 3

[30] Ole Riis and Linda Woodhead. *A sociology of religious emotion*. Oxford University Press, 2010. 2

[31] Oleksii Sidorov. Changing the image memorability: From basic photo editing to gans. In *CVPR*, pages 0–0, 2019. 1

[32] Pawel Sobkowicz, Michael Kaschesky, and Guillaume Bouchard. Opinion mining in social media: Modeling, simulating, and forecasting political opinions in the web. *Government information quarterly*, 29(4):470–479, 2012. 1

[33] Kenneth T Strongman. *The psychology of emotion: Theories of emotion in perspective*. John Wiley & Sons, 1996. 2

[34] Matthias J Wieser, Elisabeth Klupp, Peter Weyers, Paul Pauli, David Weise, Daniel Zeller, Joseph Classen, and Andreas Mühlberger. Reduced early visual emotion discrimination as an index of diminished emotion processing in parkinsons disease?–evidence from event-related brain potentials. *Cortex*, 48(9):1207–1217, 2012. 1

[35] Haitao Xiong, Hongfu Liu, Bineng Zhong, and Yun Fu. Structured and sparse annotations for image emotion distribution learning. In *AAAI*, volume 33, pages 363–370, 2019. 2, 3, 7

[36] Jufeng Yang, Dongyu She, Yu-Kun Lai, Paul L Rosin, and Ming-Hsuan Yang. Weakly supervised coupled networks for visual sentiment analysis. In *CVPR*, pages 7584–7592, 2018. 1, 3

[37] Jufeng Yang, Dongyu She, and Ming Sun. Joint image emotion classification and distribution learning via deep convolutional neural network. In *IJCAI*, pages 3266–3272, 2017. 2, 3, 7

[38] Jufeng Yang, Dongyu She, Ming Sun, Ming-Ming Cheng, Paul L Rosin, and Liang Wang. Visual sentiment prediction based on automatic discovery of affective regions. *IEEE Transactions on Multimedia*, 20(9):2513–2525, 2018. 1, 3

[39] Jufeng Yang, Ming Sun, and Xiaoxiao Sun. Learning visual sentiment distributions via augmented conditional probability neural network. In *AAAI*, pages 224–230, 2017. 2, 3, 6, 7

[40] Quanzeng You, Hailin Jin, and Jiebo Luo. Visual sentiment analysis by attending on local image regions. In *AAAI*, 2017. 3

[41] Quanzeng You, Jiebo Luo, Hailin Jin, and Jianchao Yang. Robust image sentiment analysis using progressively trained and domain transferred deep networks. In *AAAI*, 2015. 3

[42] Wei Zhang, Xuanyu He, and Weizhi Lu. Exploring discriminative representations for image emotion recognition with cnns. *IEEE Transactions on Multimedia*, 22(2):515–523, 2019. 1, 3

[43] Sicheng Zhao, Guiguang Ding, Yue Gao, Xin Zhao, Youbao Tang, Jungong Han, Hongxun Yao, and Qingming Huang. Discrete probability distribution prediction of image emotions with shared sparse learning. *IEEE Transactions on Affective Computing*, 2018. 2, 3

[44] Sicheng Zhao, Yue Gao, Xiaolei Jiang, Hongxun Yao, Tat-Seng Chua, and Xiaoshuai Sun. Exploring principles-of-art features for image emotion recognition. In *ACMMM*, pages 47–56, 2014. 3

[45] Sicheng Zhao, Hongxun Yao, Yue Gao, Rongrong Ji, Wenlong Xie, Xiaolei Jiang, and Tat-Seng Chua. Predicting personalized emotion perceptions of social images. In *ACMMM*, pages 1385–1394, 2016. 2, 3, 4, 5

[46] Sicheng Zhao, Hongxun Yao, You Yang, and Yanhao Zhang. Affective image retrieval via multi-graph learning. In *ACMMM*, pages 1025–1028, 2014. 3

[47] Xinge Zhu, Liang Li, Weigang Zhang, Tianrong Rao, Min Xu, Qingming Huang, and Dong Xu. Dependency exploitation: A unified cnn-rnn approach for visual emotion recognition. In *IJCAI*, pages 3595–3601, 2017. 1